

# Imaging the Anisotropic Nonlinear Meissner Effect in Unconventional Superconductors

Alexander P. Zhuravel,<sup>1</sup> B. G. Ghamsari,<sup>2</sup> C. Kurter,<sup>2</sup> P. Jung,<sup>3</sup> S. Remillard,<sup>4</sup>  
J. Abrahams,<sup>2</sup> A. V. Lukashenko,<sup>3</sup> Alexey V. Ustinov,<sup>3</sup> and Steven M. Anlage<sup>2,3</sup>

<sup>1</sup>*B. Verkin Institute for Low Temperature Physics and Engineering,  
National Academy of Sciences of Ukraine, UA-61103 Kharkov, Ukraine*

<sup>2</sup>*CNAM, Physics Department, University of Maryland, College Park, Maryland USA 20742-4111*

<sup>3</sup>*Physikalisches Institut and DFG-Center for Functional Nanostructures (CFN),  
Karlsruhe Institute of Technology, DE-76128 Karlsruhe, Germany*

<sup>4</sup>*Physics Department, 27 Graves Place, Hope College, Holland, MI USA 49422*

We have directly imaged the anisotropic nonlinear Meissner effect in an unconventional superconductor through the nonlinear electrodynamic response of both (bulk) gap nodes and (surface) Andreev bound states. A superconducting thin film is patterned into a compact self-resonant spiral structure, excited near resonance in the radio-frequency range, and scanned with a focused laser beam perturbation. At low temperatures, direction-dependent nonlinearities in the reactive and resistive properties of the resonator create photoresponse that maps out the directions of nodes, or of bound states associated with these nodes, on the Fermi surface of the superconductor. The method is demonstrated on the nodal superconductor  $\text{YBa}_2\text{Cu}_3\text{O}_{7-\delta}$  and the results are consistent with theoretical predictions for the bulk and surface contributions.

*Introduction* - The Meissner effect is the spontaneous exclusion of magnetic flux from the bulk of a superconductor. In the presence of a magnetic field, a superconductor must invest kinetic energy in a supercurrent flow to screen out the applied field. This reduces the free energy difference between the superconducting and normal states, resulting in a reduction in magnitude of the superconducting order parameter. This in turn changes the properties of the superconductor (e.g. magnetic penetration depth, diamagnetic moment, etc.) and is referred to as the nonlinear Meissner effect (NLME). Conventional (fully gapped) superconductors show the strongest nonlinearities near  $T_c$ , and have exponentially suppressed nonlinear response at low temperatures,  $T \ll T_c$ . Unconventional superconductors with nodes in the superconducting energy gap are expected to have a strong nonlinear Meissner effect at low temperatures, due to the nodal excitations out of the superconducting ground state [1]. In addition this nonlinear response should be anisotropic, reflecting the locations of nodes of the gap on the Fermi surface.

For a  $d_{x^2-y^2}$  gap on a circular cut of the cylindrical Fermi surface, typical of cuprate superconductors, theoretical treatments of the anisotropic NLME (aNLME) predicted a  $1/\sqrt{2}$  anisotropy at zero temperature [1, 2]. Later, the theory was re-formulated in terms of nonlinear microwave intermodulation response of a nodal superconductor [3–5], and the temperature dependence of the NLME and its anisotropy was worked out. The dependence of the superfluid density  $n_s$  on supercurrent density  $\vec{J}_s$ , for sufficiently small currents, is given by  $n_s(T, \vec{J}_s) = n_s(T)[1 - b_\Theta(T)(J_s/J_c)^2]$ , where  $J_c$  is the critical current density, and  $b_\Theta(T)$  is the nonlinearity coefficient dependent on the direction (angle  $\Theta$ ) of  $\vec{J}_s$  [3]. It was found that the anisotropy in the NLME of cuprates

is weak at high temperatures, and only becomes significant for  $T/T_c < 0.6$  [4]. In addition, it was found that  $b_\Theta(T)$  is expected to grow as  $1/T$  for  $T/T_c < 0.2$  [3], before crossing over to another temperature dependence, depending on the purity of the material [2, 5, 6].

Early experiments to detect the aNLME of cuprates through transverse magnetization [7, 8], magnetic penetration depth [9–11], and surface impedance [12] measurements did not establish conclusive evidence of the effect [6]. Later, sensitive nonlinear microwave measurement techniques established the existence of the NLME in cuprates from the temperature dependence of the intermodulation power at low temperatures [13–15], although the anisotropy of the effect was not measured. Although other thermodynamic measurements have shown evidence of an anisotropic energy gap in various superconductors [16–18], there are no unambiguous measurements of the aNLME in cuprates, to our knowledge. In contrast to quasiparticle transport methods [16–18], the present method utilizes the bulk superfluid response to identify the nodal directions [19].

An additional contribution to the NLME in unconventional superconductors arises from Andreev bound states (ABS) [20], created, for example, on the (110) surface of a  $d_{x^2-y^2}$  superconductor. These states give rise to a *paramagnetic* contribution to the screening [21]. For cuprates, (110) interfaces occur at twin boundaries, which are formed spontaneously during epitaxial film growth. The NLME associated with ABS has been established by tunneling [22], and penetration depth measurements [23, 24], for example. Theory by Zare, Dahm and Schopohl (ZDS) predicts an aNLME associated with ABS having a strong temperature dependence at low temperatures, eventually dominating that due to nodal excitations [25].

Here we establish a new method to both quantitatively measure and image the aNLME from nodes in the superconducting gap using a novel RF resonant technique combined with laser scanning microscopy.

**Experiment** - We employ a self-resonant superconducting structure based on a thin film Archimedean spiral geometry. The spiral has an inner diameter of 4.4 mm, an outer diameter of 6 mm, and consists of 40 turns of nominally 10  $\mu\text{m}$  width thin film stripe with 10  $\mu\text{m}$  spacing, winding continuously from the inner to outer radii with Archimedean form (see the schematic in Fig. 1(a)). The structure has considerable inductance and capacitance, making it a compact self-resonant meta-atom for use in superconducting metamaterials [26, 27]. When made from superconducting materials such as Nb and  $\text{YBa}_2\text{Cu}_3\text{O}_{7-\delta}$  (YBCO), the spiral has a fundamental resonance in the vicinity of 75 MHz, and many overtones extending above 1 GHz. The distribution of standing wave currents on the spiral in the first few modes are well approximated as those of a resonant vibrating string held fixed at both ends, and then wrapped into a spiral, as verified by detailed laser scanning microscope (LSM) imaging [28–30]. A unique property of the resonant spiral is the fact that currents flow in a uniform manner around the Fermi surface of the superconductor.

The epitaxial and in-plane oriented YBCO films on  $\text{LaAlO}_3$  (LAO) were deposited by *in-situ* off-axis magnetron sputtering to a thickness of 300 nm [31]. Similar YBCO films on  $\text{CeO}_2$  buffered sapphire and on MgO were deposited by thermal coevaporation to a thickness of 300 nm and 700 nm, respectively [32]. The 200 nm thick Nb films were deposited on quartz substrates at room temperature by RF sputtering [26, 28]. All films were patterned into spiral resonators by contact photolithography and either wet or dry chemical etching.

The LSM operates by scanning a focused laser spot (wavelength 640 nm) over the surface of the spiral while it is excited near its RF resonance with excitation and pickup loops above and below the plane of the film. Details of the RF and laser excitations of the spirals have been previously published [26, 28–30]. The spiral develops a photoresponse due to pair-breaking and localized heating, producing a change in its resonant frequency and quality factor [33, 34]. The laser intensity is modulated at 100 kHz, and the changes in RF transmission at a fixed frequency are phase sensitively detected, resulting in a photoresponse (PR) signal consisting of both a magnitude and phase. The peak laser intensity can be varied between 150  $\mu\text{W}$  and 1.6 mW. The laser spot (about 20  $\mu\text{m}$  diameter) is scanned over the sample to create a two-dimensional PR image.

The aNLME is expected to create the following PR contrast [3, 35]. For a  $d_{x^2-y^2}$  gap on a circular Fermi surface one expects  $\text{PR} \sim 1 + \sin^2(2\Theta)$  with  $\Theta = 0$  along the Cu-O-Cu bond direction of YBCO (see Fig. 1(a)). In addition, the PR amplitude should vary as  $1/T^2$  for

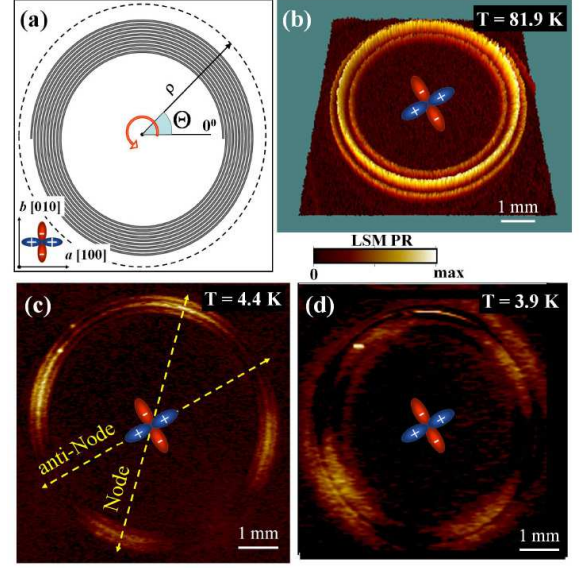


FIG. 1. a) Schematic diagram of spiral geometry, definition of radial ( $\rho$ ) and angular ( $\Theta$ ) coordinates, and directions of the crystallographic  $a$ - and  $b$ -directions, along with the orientation of the  $d$ -wave gap in YBCO. b)-d) LSM photoresponse images of a YBCO/LAO spiral resonator in the third harmonic mode at temperatures of b) 81.9 K, c) 4.40 K, d) 3.90 K. Also shown is the  $d$ -wave gap orientation as determined from twin domain boundary directions in the substrate.

$T/T_c < 0.2$  and  $J_{RF}/J_c < T/T_c$ , where  $J_{RF}$  is the RF current density induced in the sample. It is also expected that the LSM PR is proportional to RF power and proportional to the intensity of the laser light. As deduced from ZDS, the contribution to LSM PR from ABS should be centered on (110) surfaces of the material, have a stronger temperature dependent  $\text{PR} \sim 1/T^4$ , have the opposite sign of PR from the nodal aNLME (due to the paramagnetic nature of the ABS), and be a linear function of RF and laser power up to RF fields on the order of a few mT [25].

**Results** - Figure 1 shows LSM PR images of a single YBCO/LAO spiral in a resonant mode at three different temperatures, 81.9 K, 4.4 K and 3.9 K. The image is of the third harmonic mode and shows three nearly circular distinct bands of enhanced PR, corresponding to the three half-wavelengths of current distributed over the 40 turns of superconducting wire [28–30]. One notes that the PR is isotropic in its angular distribution around the spiral at 81.9 K (Fig. 1(b)). However, the LSM PR image of the same mode at 4.40 K (Fig. 1(c)) shows four distinct enhancements of PR at regular angular intervals around the spiral. As the sample is cooled further (below about 4.30 K for this particular sample), a new set of enhanced-PR features are observed in Fig. 1(d), but now rotated 45° relative to those at 4.40 K. Images of Nb spirals of nominally identical geometry in the same mode do not

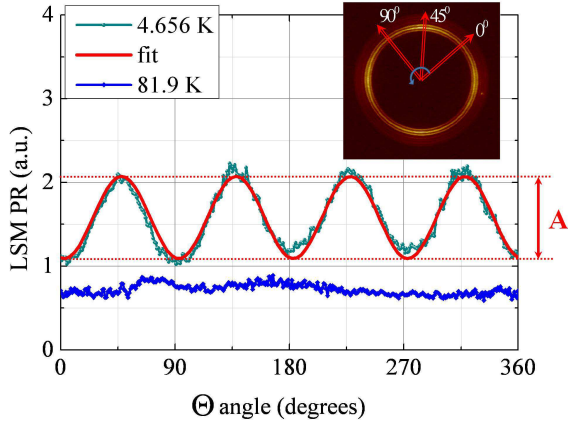


FIG. 2. Plot of radially-integrated and unwrapped photoresponse (PR) vs. angle on the YBCO/LAO spiral at 81.9 K and 4.66 K, along with a fit of the low-temperature integrated  $PR(\Theta)$  to the simple d-wave angular dependence. Inset shows PR image of YBCO/LaAlO<sub>3</sub> thin film spiral resonator taken at a temperature of 4.656 K in the 7<sup>th</sup> mode at 450.22 MHz.

show this anisotropic PR at any temperature below the transition temperature. The above anisotropy and rotation behavior is observed to hold for the YBCO/LAO spiral excited into all modes, from the fundamental through the 8<sup>th</sup> mode (the highest examined).

Figure 2 shows the radially( $\rho$ )-integrated PR as a function of angle for a YBCO/LAO thin film spiral resonator taken at a temperature of 4.66 K in the 7<sup>th</sup> mode at 450.22 MHz, shown in the inset. The zero-angle (Cu-O-Cu bond) direction was determined from the visible twinning structure of the LAO substrate. Utilizing the fact that the YBCO film was grown *epitaxially* and in-plane oriented on LAO, the observation that the PR maxima are aligned along the linear twin domain structures in the substrate, and the fact that the twin boundaries are aligned at 45° to the Cu-O-Cu bond direction [36], we deduced that the  $\Theta = 0$  direction is at 45° to the twin domain structure of the substrate. Figure 2 shows a fit of the data to  $PR(\Theta) = 1 + A \sin^2(2\Theta)$ , resulting in a fit value  $A = 1.05 \pm 0.02$ , close to the value of 1 expected for a simple  $d_{x^2-y^2}$  gap on a circular Fermi surface.

The PR images in the ‘rotated’ state at lower temperatures (Fig. 1(d)) also show 4-fold character, but are relatively diffuse in appearance, and display dramatically stronger PR as the temperature is lowered. To understand these properties, we examine the temperature dependence and phase of the photoresponse along the nodal ( $\Theta = \pi/4$ ) and anti-nodal ( $\Theta = 0$ ) directions of the superconducting gap. Figure 3 shows a plot of PR magnitude vs. temperature for nodal and anti-nodal regions of a YBCO/sapphire spiral resonator. In the nodal direction the PR is of significant magnitude at a temperature of 6.6 K, but decreases in magnitude as temperature is lowered. The PR goes to near-zero levels

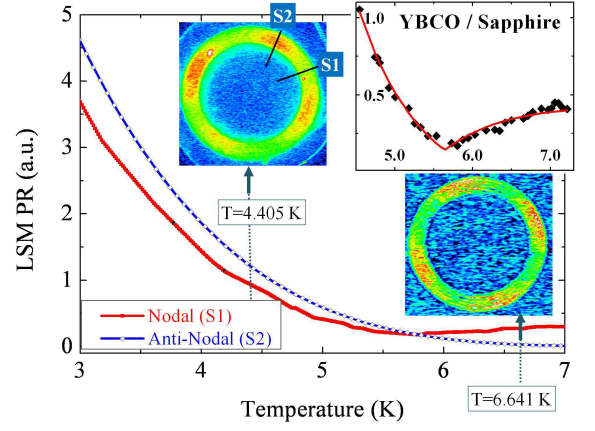


FIG. 3. Plot of temperature dependence of photoresponse (PR) magnitude taken at nodal and anti-nodal locations in a YBCO/sapphire spiral resonator. The anti-nodal PR has opposite sign to the nodal PR above the crossover temperature (about 5.5 K). Inset shows temperature dependence of nodal PR magnitude near its crossover temperature, along with a fit to the form predicted by ZDS. Other insets show LSM PR magnitude images of YBCO/sapphire below (4.405 K) and above (6.641 K) its crossover temperature at 546.555 MHz. The phase of the PR in these images differ by  $\pi$ , corresponding to a sign reversal of the response.

and changes phase by  $\pi$  radians at a point that we call the ‘crossover temperature.’ Below this temperature the nodal PR magnitude increases dramatically. In the anti-nodal directions the PR is found to be smaller than the nodal PR at 6.6 K, but increases monotonically in magnitude with decreasing temperature, and has the same phase as the nodal PR below the crossover temperature.

A fit of the PR to the expected temperature dependence of nodal PR (temperature derivative of Eq. (16) of Ref. 25), namely  $PR \sim A/T^2 - B/T^4$  (first term due to nodal NLME and second due to ABS NLME) [25], is shown in the inset of Fig. 3 for a YBCO/sapphire sample. The data is consistent with the predicted temperature dependence around the crossover temperature.

In all of these experiments we have verified that the LSM PR in the nodal direction is proportional to both RF power and to laser intensity. The LSM PR in the anti-nodal direction is linear at low laser powers, but becomes strongly nonlinear at higher laser powers. YBCO films grown on other substrates (MgO and sapphire) show the same general behavior described above as the samples on LAO. The insets of Fig. 3 shows images of the YBCO/sapphire sample below (4.405 K) and above (6.641 K) the crossover temperature for this sample. We find that the PR maxima are aligned along the nodal directions of YBCO at higher temperatures, and then show a ‘rotation’ by 45° at lower temperatures, although the crossover temperature is sample dependent (approximately 4 - 5 K for YBCO/LAO and 5 - 7 K for YBCO/MgO and YBCO/sapphire). This sample de-

pendence may be associated with different abundances of (110) surfaces and twinning in each sample.

*Discussion* - A reorientation of specific heat oscillations with magnetic field direction (qualitatively similar to the crossover observed here) has been reported in superconductors with anisotropic order parameters [37, 38]. However, specific heat measures the low-energy quasiparticle density of states [39] while our measurements probe the superfluid response and involve no DC magnetic field or vortices. Therefore we do not believe that quasiparticle transport phenomena are the origin of the crossover observed in this paper. On the other hand, the observed sign difference of LSM PR between the nodal and anti-nodal directions above the crossover temperature is consistent with the ZDS prediction for the NLME due to ABS [25]. The strong and monotonic temperature dependence of PR observed along the (110) directions of the film are also consistent with the ZDS prediction. The observed crossover temperature (4 K to 7 K) is on the order of that predicted by ZDS, namely  $T_c/\kappa^{1/2} \sim 10$  K, where  $\kappa$  is the Ginzburg-Landau parameter. Together, these results confirm the basic predictions of ZDS for the relative contributions of the nodal and ABS contributions to the NLME. Note that the use of thin film superconducting spiral resonators that expose many different crystallographic directions, and which have a large surface-to-volume ratio, accentuates the contribution of ABS to the photoresponse.

In order to verify the above interpretation of the data, a number of potential artifacts and other interpretations of the PR images have been systematically explored. First is the possibility of anisotropic PR being created by the irregularly-shaped excitation and RF pickup loops. The anisotropic PR did not change when the excitation loop was rotated relative to the sample. In addition, the anisotropic PR pattern rotated when the sample was rotated relative to the loops. We do not observe a significant degree of PR anisotropy in Nb spirals measured under similar conditions.

A second concern is that the PR temperature dependence arises from a growing thermal boundary resistance,  $R_{bdy} \sim 1/T^3$ , between the thin film superconductor and the dielectric substrate [40]. However the strong temperature dependence is not observed in Nb/quartz samples, eliminating most of the cryostat components from generating this response. All YBCO samples (on LAO, MgO and sapphire) show the strong PR temperature dependence at low temperatures. Nevertheless, we do believe that a thermal blockade may set in for the YBCO/LAO samples at low temperatures ( $< 3$  K), resulting in diffuse PR images. This interpretation was independently verified through measurements of the PR thermal relaxation time as a function of temperature.

A third concern is that the twinned structure of the LAO substrate traps heat and channels it in specific directions, giving rise to the observed anisotropy. How-

ever, we observe the same anisotropy on YBCO/MgO and YBCO/sapphire films that do not have twinned substrates. The apparent rotation of the PR by  $45^\circ$  in a narrow temperature range in all of the YBCO samples also argues against a substrate-induced anisotropy. Next is the concern that the shape of the substrate dictates the anisotropy of the PR in the spiral. Numerical simulations of localized heating of a spiral on a square substrate under conditions similar to those of our YBCO samples showed a temperature anisotropy of only 1 part in 1000 imposed by the shape of the substrate, whereas the observed anisotropy is on the order of 50%. Finally is the concern that defects in the lithographic pattern of the spiral (namely shorts between wires or opens) will create the anisotropic PR. We find that all YBCO spirals, from those with near-perfect lithography to those with defective patterns, all show the anisotropy and temperature dependent properties described above.

*Conclusions* - We have measured and imaged the anisotropic nonlinear Meissner effect in an unconventional superconductor arising from both bulk and surface mechanisms. Our results are in detailed agreement with aNLME theoretical predictions based on both nodal and ABS contributions to the photoresponse. This establishes a new gap spectroscopy tool that is sensitive to nodes in the superconducting gap accessed by currents flowing in the plane of the material, and can detect gap nodes directly, or indirectly through Andreev bound states, through their influence on the in-plane electrodynamics in the superconducting state.

*Acknowledgements* We thank D. J. Scalapino, I. Mazin, and V. Yakovenko for helpful discussions. The work at Maryland was supported by ONR Grants No. N000140811058 and No. 20101144225000, the US DOE DESC 0004950, the ONR AppEl Center, Task D10 (N000140911190), and CNAM. The work in Karlsruhe is supported the Deutsche Forschungsgemeinschaft (DFG) and the State of Baden-Württemberg through the DFG-CFN, and a NASU program on Nanostructures, Materials and Technologies. S.M.A. acknowledges sabbatical support from the CFN at KIT.

- 
- [1] S. K. Yip and J. A. Sauls, Phys. Rev. Lett. **69**, 2264 (1992).
  - [2] D. Xu, S. K. Yip, and J. A. Sauls, Phys. Rev. B **51**, 16233 (1995).
  - [3] T. Dahm and D. J. Scalapino, J. Appl. Phys. **81**, 2002 (1997).
  - [4] T. Dahm and D. J. Scalapino, Appl. Phys. Lett. **69**, 4248 (1996).
  - [5] T. Dahm and D. J. Scalapino, Phys. Rev. B **60**, 13125 (1999).
  - [6] M. R. Li, P. J. Hirschfeld, and P. Wolfle, Phys. Rev. Lett. **81**, 5640 (1998).
  - [7] J. Buan, *et al.*, Phys. Rev. Lett. **72**, 2632 (1994).

- [8] A. Bhattacharya, *et al.*, Phys. Rev. Lett. **82**, 3132 (1999).
- [9] A. Carrington, *et al.*, Phys. Rev. B **59**, 14173 (1999).
- [10] C. P. Bidinosti, *et al.*, Phys. Rev. Lett. **83**, 3277 (1999).
- [11] K. Halterman, O. T. Valls, and I. Zutic, Phys. Rev. B **63**, 180405 (2001).
- [12] A. Maeda, *et al.*, Phys. Rev. Lett. **74**, 1202 (1995).
- [13] G. Benz, *et al.*, Physica C **356**, 122 (2001).
- [14] D. E. Oates, S. H. Park, and G. Koren, Phys. Rev. Lett. **93**, 197001 (2004).
- [15] K. T. Leong, J. C. Booth, and S. A. Schima, IEEE Trans. Appl. Supercond. **15**, 3608 (2005).
- [16] I. Vekhter, *et al.*, Phys. Rev. B **59**, R9023 (1999).
- [17] H. Aubin, *et al.*, Phys. Rev. Lett. **78**, 2624 (1997).
- [18] T. Park, *et al.*, Phys. Rev. Lett. **90**, 177001 (2003).
- [19] I. Žutić and O. T. Valls, Phys. Rev. B **56**, 11279 (1997).
- [20] C.-R. Hu, Phys. Rev. Lett. **72**, 1526 (1994).
- [21] M. Fogelström, D. Rainer, and J. A. Sauls, Phys. Rev. Lett. **79**, 281 (1997).
- [22] M. Aprili, E. Badica, and L. H. Greene, Phys. Rev. Lett. **83**, 4630 (1999).
- [23] H. Walter, *et al.*, Phys. Rev. Lett. **80**, 3598 (1998).
- [24] A. Carrington, *et al.*, Phys. Rev. Lett. **86**, 1074 (2001).
- [25] A. Zare, T. Dahm, and N. Schopohl, Phys. Rev. Lett. **104**, 237001 (2010).
- [26] C. Kurter, J. Abrahams, and S. M. Anlage, Appl. Phys. Lett. **96**, 253504 (2010).
- [27] S. M. Anlage, J. Optics **13**, 024001 (2011).
- [28] C. Kurter, *et al.*, IEEE Trans. Appl. Supercond. **21**, 709 (2011).
- [29] C. Kurter, *et al.*, Phys. Rev. B **84**, 104515 (2011).
- [30] A. P. Zhuravel, *et al.*, Phys. Rev. B **85**, 134535 (2012).
- [31] D. W. Face, *et al.*, IEEE Trans. Appl. Supercond. **7**, 1283 (1997).
- [32] [http://www.theva.com/user/eesy.de/theva.biz/dwn/Datasheet\\_Coatings.pdf](http://www.theva.com/user/eesy.de/theva.biz/dwn/Datasheet_Coatings.pdf)
- [33] A. P. Zhuravel, *et al.*, Low Temp. Phys. **32**, 592 (2006).
- [34] A. P. Zhuravel, *et al.*, J. Appl. Phys. **108**, 033920 (2010).
- [35] D. J. Scalapino, private commun.
- [36] Y. M. Wang, *et al.*, Phil. Mag. Letts. **88**, 481 (2008).
- [37] K. An, *et al.*, Phys. Rev. Lett. **104**, 037002 (2010).
- [38] B. Zeng, *et al.*, Nat. Commun. **1**, 112 (2010).
- [39] A. B. Vorontsov, I. Vekhter, Phys. Rev. B **75**, 224501 (2007).
- [40] E. T. Swartz and R. O. Pohl, Rev. Mod. Phys. **61**, 605 (1989).